Silurian horseshoe crab illuminates the evolution of arthropod limbs

Derek E. G. Briggs[a,1], Derek J. Siveter[b,c], David J. Siveter[d], Mark D. Sutton[e], Russell J. Garwood[f], and David Legg[e]

[a]Department of Geology and Geophysics, and Yale Peabody Museum of Natural History, Yale University, P.O. Box 208109, New Haven, CT 06520-8109; [b]Geological Collections, University Museum of Natural History, Oxford OX1 3PW, United Kingdom; [c]Department of Earth Sciences, University of Oxford, South Parks Road, Oxford OX1 3AN, United Kingdom; [d]Department of Geology, University of Leicester, Leicester LE1 7RH, United Kingdom; [e]Department of Earth Sciences and Engineering, Imperial College London, London SW7 2BP, United Kingdom; and [f]School of Materials, and School of Earth, Atmospheric and Environmental Sciences, University of Manchester, Manchester M13 9PL, United Kingdom

Edited by Andrew H. Knoll, Harvard University, Cambridge, MA, and approved August 16, 2012 (received for review April 9, 2012)

The basic arrangement of limbs in euarthropods consists of a uniramous head appendage followed by a series of biramous appendages. The body is divided into functional units or tagmata which are usually distinguished by further differentiation of the limbs. The living horseshoe crabs are remnants of a much larger diversity of aquatic chelicerates. The limbs of the anterior and posterior divisions of the body of living horseshoe crabs differ in the loss of the outer and inner ramus, respectively, of an ancestral biramous limb. Here we report a new fossil horseshoe crab from the mid-Silurian Lagerstätte in Herefordshire, United Kingdom (approximately 425 Myr B.P.), a site that has yielded a remarkably preserved assemblage of soft-bodied fossils. The limbs of the new form can be homologized with those of living *Limulus*, but retain an ancestral biramous morphology. Remarkably, however, the two limb branches originate separately, providing fossil evidence to suggest that repression or loss of gene expression might have given rise to the appendage morphology of *Limulus*. Both branches of the prosomal limbs of this new fossil are robust and segmented in contrast to their morphology in Cambrian arthropods, revealing that a true biramous limb was once present in chelicerates as well as in the mandibulates.

Xiphosurida | origin of limb morphology | Herefordshire Lagerstätte

Horseshoe crabs (Xiphosura), together with the extinct eurypterids (sea scorpions) and chasmataspidids, represent an aquatic grade of chelicerates in contrast to the terrestrial arachnids (1, 2). Horseshoe crabs are united by several characters: a prosoma with ophthalmic ridges and a cardiac lobe, and an opisthosoma with a reduced first segment and a defined axial region (3). Among horseshoe crabs the Xiphosurida, which includes the living forms, are characterized by a fused opisthosoma (4); the oldest example is an undescribed taxon with preserved appendages from the Lower Ordovician (Tremadocian-Floian) of Morocco (5). Synziphosurines are a paraphyletic group low on the stem of Xiphosura with an unfused opisthosoma composed of nine to 11 segments (4). Synziphosurines also first appear as an undescribed taxon in the Lower Ordovician of Morocco, although they likely originated even earlier (5), and range into the Lower Carboniferous (Namurian) (6). The interrelationships of synziphosurines are uncertain: limbs are only known in the Silurian *Offacolus kingi* from Herefordshire, England (7, 8), here shown to be a synziphosurine, and *Venustulus waukeshaensis* from Waukesha, Wisconsin, USA (9), and the Devonian *Weinbergina opitzi* from Hunsrück, Germany (10).

Results

Dibasterium durgae is a new genus and species of synziphosurine from the Herefordshire Lagerstätte (11, 12), a volcaniclastic deposit of mid-Silurian (late Wenlock) age in Herefordshire. *Dibasterium* is preserved, like other fossils from this locality (13), as a three-dimensional calcitic void fill in a carbonate concretion. The name refers to the remarkable biramous prosomal limbs (*dibamos*: on two legs; *mysterium*: mystery) and to Durga, the Hindu goddess with many arms. The material is a single specimen, the holotype OUMNH C.29640, registered at the Oxford University Museum of Natural History (Fig. 1, Fig. S1, Movie S1).

Diagnosis. Head shield semioval, smooth, lacking external evidence of a differentiated ophthalmic area; 11 unfused opisthosomal tergites, the first reduced; telson terminating in two short spines. Chelicera elongate, flexible; prosomal limbs 2–5 biramous, both rami robust, segmented, inserting separately; limb six uniramous, similar to preceding endopods; limb seven short with spine-fringed flap; six lamellate opisthosomal limbs.

Description. The body is divided into three tagmata, a prosoma bearing a head shield and an unfused opisthosoma divided into a preabdomen and postabdomen (Fig. 1 *A* and *B*). The total length is 23.2 mm excluding appendages; the maximum width of the prosoma is 9.2 mm.

The head shield is incomplete oval in outline with a slightly procurved posterior margin (Fig. 1*E*); it is similar in length and width, and semicircular in anterior view (Fig. 1*H*). The surface is smooth, with no evidence of eyes or an ophthalmic area. The prosoma bears seven pairs of appendages (Fig. 1 *B* and *F*). The first pair (chelicerae) insert close together (Fig. 1*F*) and they are preserved extending back along the axis before curving antero-dorsally at their distal extremity (the length is approximately 75% that of the head shield). Three probable segment boundaries can be discerned distally; the curvature (Fig. 1*C*) of the rest of the chelicera suggests that it is flexible and composed of numerous podomeres, but their boundaries cannot be determined. The chelicera terminates in a small chela.

Appendages 2 to 6 project just beyond the head shield (Fig. 1 *F* and *H*). Appendages 2 to 5 are biramous (Fig. 1 *F* and *I*). The inner rami (endopods) insert in a series posterior of the chelicera, surrounding a raised central area occupied by the mouth. The outer rami insert along the outer margin of the ventral body wall. There is no evidence that these two rami were connected by an elongate limb base like the coxa in *Limulus*. Nonetheless the rami clearly represent elements of the same limb rather than successive limbs alternating in morphology. The morphology of these four appendages is essentially identical (Fig. 1 *F*, *J*, *L*, and *M*) and evidence from all of them allows the position of the podomere boundaries to be interpreted.

The limb base is subtriangular, laterally compressed, and gnathobasic. The endopod comprises six podomeres plus a

Author contributions: Derek J.S., David J.S., D.E.G.B., and M.D.S. designed research; Derek J.S., David J.S., D.E.G.B., M.D.S., R.J.G., D.L. performed research; and D.E.G.B. wrote the paper.

The authors declare no conflict of interest.

This article is a PNAS Direct Submission.

[1]To whom correspondence should be addressed. E-mail: derek.briggs@yale.edu.

This article contains supporting information online at www.pnas.org/lookup/suppl/doi:10.1073/pnas.1205875109/-/DCSupplemental.

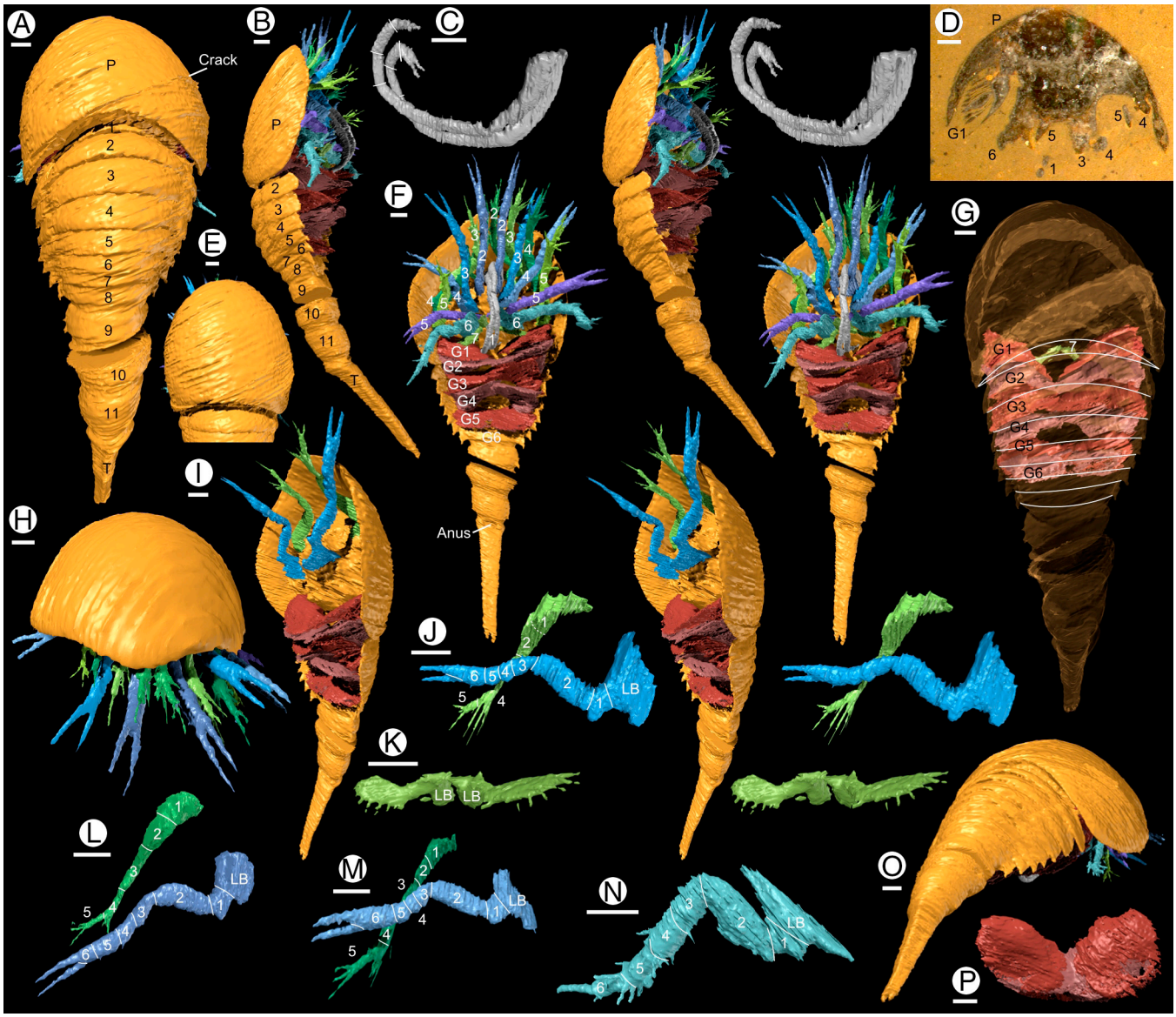

Fig. 1. Holotype of *Dibasterium durgae* gen. et sp. nov.: (*A*–*C*, *E*–*P*) "virtual" reconstructions; (*D*) specimen in rock. (*A*) Dorsal, (*B*) lateral (stereo-pair), and (*C*) left lateral view of paired antenniform chelicera (stereo-pair), (*D*) specimen prior to reconstruction; surface is along original crack labeled in (*A*), (*E*) dorsal view of head shield, (*F*) ventral view (stereo-pair), (*G*) dorsal view, anterior prosomal appendages removed, head shield rendered transparent to show position of 7th appendage and gills, tergite boundaries of preabdomen outlined, (*H*) anterior view, (*I*) oblique ventral view, prosomal limbs removed apart from limb 3, to show separate insertion of endopod and exopod (stereo-pair), (*J*, *L*, *M*) lateral view of left prosomal appendages 3 (stereo-pair), 2 and 4, endopod "overlying" exopod, (*K*) posterior ventral view of appendage 7=chilaria (stereo-pair), (*N*) lateral view of right prosomal appendage 6, (*O*) posterior oblique view, (*P*) anterior view of gills. Abbreviations: G1-6, opisthosomal limbs (gills); L B, limb base; P, prosoma; T, telson. Numbers refer to opisthosomal tergites, prosomal limbs, and podomeres, as appropriate.

terminal claw (Fig. 1 *J*, *L*, and *M*). The endopod is suboval in cross-section (weakly compressed laterally). The first podomere is short with a ventral projection. The second lies at a high angle to the first and is the longest. The remainder of the limb flexes downward through approximately 60°. Podomeres 3 to 5 are short and bulge slightly on their lower margin. Podomere 6 is followed by a claw, either one or both of the fingers presumably articulated proximally. The podomeres of the endopod (see ref. 10) are interpreted as trochanter, femur, patella, tibia, basitarsus, telotarsus, and apotele [=pretarsus: (14)]. The outer ramus (Fig. 1 *J*, *L*, and *M*) comprises five podomeres and is shorter than the endopod. The basal division is here termed podomere 1: it is short and broad at the base, tapering distally. Podomere 2 is the longest and directed down at approximately 25° to the first. Podomeres 3 and 4 are similar in length. A small spine projects laterally from the distal extremity of podomere 3. Podomere 4 projects ventrally into an array of five spines whereas podomere 5 terminates in three spines.

Appendage 6 (Fig. 1*N*) consists of the limb base and endopod alone. Podomere 1 is short. Podomere 2 is the longest, and is oriented almost parallel to the limb base. The limb flexes through approximately 90°. Podomeres 3 to 5 taper and are fringed distally by spines. Podomere 6 bears a single elongate, slender projection; there is no evidence of a chela (the left limb of the pair is incomplete distally). Appendage 7 (Fig. 1*K*) is small relative to the other limbs. The limb base projects anteroventrally forming a barrier posterior to the mouth. A single short ramus consists of a small oval flap fringed by short spines which is borne by a narrow shaft that may or may not be segmented.

The opisthosoma consists of 11 somites and a telson (Fig. 1 *A* and *B*). Eight somites make up the preabdomen which, like the prosoma, is highly vaulted with a wide axis (Fig. 1 *A*, *B*, and *O*).

The first tergite (Fig. 1 *A*, *G*, and *O*) is narrow transversely and lacks pleurae; it extends anteriorly beneath the head shield where it is largely concealed. Tergites 2 to 8 (Fig. 1 *A*, *B*, and *G*) are smoothly curved in transverse section, the pleurae delimited from the axis by a shallow axial furrow which constitutes the only surface relief. Tergites 2 to 4 are longer than the rest. The pleurae extend postero-laterally into an angle that becomes more spine-like in the more posterior tergites (Fig. 1*O*).

The preabdomen bears six pairs of "gills" (Fig. 1 *B*, *F*, *G*, *I*, and *P*) consisting of stacks of lamellae. When the gills are viewed through the head shield (Fig. 1*G*), the axial part of gill 1 corresponds in position to the boundary between opisthosomal tergites 2 and 3 and presumably belongs to opisthosomal somite 2. There is no evidence that gill 1 is modified (as a genital operculum, for example). The gills are wider (transversely) than deep (dorsoventrally). Individual gill lamellae are evident ventrally (Fig. 1*B*): extrapolation suggests that there were 20–30 in the more anterior gills. The lamellae diminish in size posteriorly within each gill (Fig. 1*F* and *I*). The left and right gills of the first pair are separated medially but those of successive gills meet or overlap slightly. The gills appear to insert near the axis of the opisthosoma, but the nature of the attachment is unknown. Opisthosomal somite 8 is apodous (Fig. 1 *B*, *F*, and *G*); it is semicircular in transverse section rather than concave ventrally like the somites in front of it.

The postabdomen (Fig. 1 *A*, *B*, *F*, and *O*) consists of three enclosed segments (9–11) and a telson. Segments 9–11 are semicircular in transverse section. Posterolateral spines (evident on the left side) are present at the boundary between the dorsal and ventral surfaces indicating the separation of tergite and sternite. The narrowing between the segments presumably represents areas of flexible cuticle that permitted movement.

No trace of the gut is preserved. A small depression on the ventral side at the anterior of the telson represents the position of the anus (Fig. 1 *F* and *I*). A thickened rim runs round the telson behind the anus; beyond this the telson is triangular in section (Fig. 1*O*). The telson terminates in two small projections (Fig. 1 *A*, *F*, *I*, and *O*).

Discussion

A New Genus. The unfused opisthosoma indicates that the affinities of *Dibasterium* lie with the synziphosurines (Fig. 2, Fig. S1); Xiphosurida are characterized by a fused opisthosoma (4). The interrelationships of synziphosurines are uncertain: limbs are only known in *Offacolus kingi* (7, 8), *Venustulus waukeshaensis* (9), and *Weinbergina opitzi* (10). The generic identity of synziphosurines is therefore based on the morphology of the dorsal exoskeleton. *Dibasterium* shows most similarity to the Weinberginidae (10), but there is no evidence that *Weinbergina* has a microtergite (it only has 10 opisthosomal segments) and a restudy of *Legrandella* is necessary to confirm that it has 11 opisthosomal segments. All described synziphosurines show evidence of lobes on the prosomal carapace surface (4) whereas *Dibasterium* is smooth. Thus *Dibasterium* is described as a new genus.

The Nature of the Limbs. Horseshoe crabs, such as living *Limulus*, are characterized by two homonomous series of limbs (in the prosoma and opisthosoma), their biphasic development presumably under the control of *Hox* genes (14). *Offacolus* (7, 8) has a strikingly similar prosomal appendage arrangement to that in *Dibasterium*. In the light of its position stemward of *Dibasterium* and *Weinbergina* (Fig. 2, Fig. S1) *Offacolus* can also be considered a synziphosurine, albeit with an aberrant trunk morphology (the posterior part of the opisthosoma is fused) that may be paedomorphic. The limbs of all these fossil taxa appear homologous with those in *Limulus* (15) prompting a consideration of their significance for the evolution of limbs in Chelicerata.

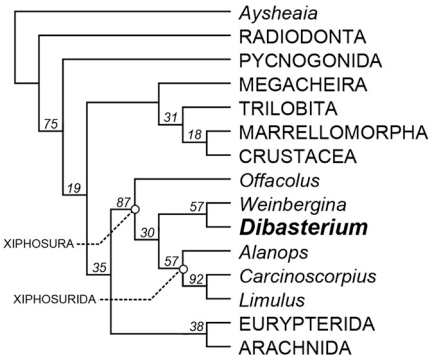

Fig. 2. Cladogram showing the position of *Dibasterium durgae* among Xiphosura (horseshoe crabs). *Offacolus*, *Dibasterium*, and *Weinbergina* represent the paraphyletic synziphosurines that lie stemward of Xiphosurida, which includes the living *Carcinoscorpius* and *Limulus*. Single MPT (most parsimonious tree) of 13.03 steps (CI = 0.760; RI = 0.867) produced using traditional search options with a TBR algorithm and implied weighting ($k = 3$). Numbers above nodes are GC support values. See *SI Text* for more details.

The evidence of Hox gene expression (16) and the deutocerebral innervation of the chelifore in pycnogonids, which corresponds to the chelicera in euchelicerates (17), show that the chelicera is equivalent to the antennule (first antenna) in other arthropod groups even though the two are very different in morphology. The chelicera of *Dibasterium* is elongate and apparently flexible, and represents a morphology more antenniform than in other chelicerates.

The outer ramus of limbs 2–5 in both *Dibasterium* and *Offacolus* is robust and segmented in a manner similar to the endopod and is here interpreted as a true exopod (it is unlikely that the flabellum on limb 6 in *Limulus* or the tendril-like outer ramus on this limb in *Offacolus* are homologous). In the light of the morphology of *Dibasterium*, we reinterpret the inner and outer rami of limbs 2–5 in *Offacolus* as also inserting separately; we previously noted (see legend to Fig. 4 in ref. 8) that the two rami had not been "unambiguously shown to be a single unit." The positional separation of the rami in prosomal limbs 2–5 of *Dibasterium* and *Offacolus* reflects a stage in the loss of the exopod of the prosomal limbs of horseshoe crabs, a loss already reached by limb 6 in *Dibasterium*. Limb 7 in both these taxa, on the other hand, is very different and may be homologous to the chilaria in *Limulus*. All the prosomal limbs are similar and uniramous in *Weinbergina* (Early Devonian) (10) where the exopod has apparently been lost.

Limb Development. The separation of the two rami in limbs 2 to 5 in *Dibasterium*, as well as the absence of the exopod in limb 6, suggest a developmental explanation for the loss of the outer ramus in the prosomal limbs of horseshoe crabs. *Distal-less* (*Dll*) expression has been documented in *Limulus* in association with the prosomal limbs, although it also plays a role in the development of sensory organs and the central nervous system (18) and is not always associated with arthropod limbs (19). Marked *Dll* expression coincides with the position of the endopods in limbs 1–5 in *Limulus*. Small transitory expressions of *Dll* are also present in limbs 2–5 in the early embryo, in a position similar to the outer ramus in *Dibasterium*, but they do not form outgrowths (see Fig. 3*A* in ref. 18). These expression domains in *Limulus* have been interpreted as vestiges of exites [equivalent to the flabellum of limb 6: (see refs. 18, 20)] or of exopods (14, 15). There is no such transitory expression in association with the chelicera (18), which is fundamentally uniramous. The transient *Dll* expression domains flanking the pedipalpal and walking limb buds of *Limulus* embryos could mark the former positions of the outer ramus. However, the regulation of these domains is unknown; the expression domains of prosomal Hox genes have not been

reported for *Limulus*. The evolutionary loss of outer rami following the separation of the rami could result from repression and/or loss of appendage-patterning gene domains, but both this set of homologies and the mechanism of ramus reduction require further study.

In developmental terms the biramous limbs of some Cambrian arthropods have been interpreted as endopods with exites [such a limb may have originated by fusion of lobopods and gill flaps: (21, 22)] rather than truly biramous appendages where endopod and exopod arose by splitting of the main limb axis (20). Under this model the flabellum on limb 6 of *Limulus* is an exite and a true biramous limb only arises in the mandibulates (20). However, the presence of a robust, segmented outer ramus (14, 15) in the chelicerates *Dibasterium* and *Offacolus*, which is presumably the result of splitting of the limb, indicates that a "true" biramous limb was also present in the chelicerates. The appearance of the biramous limb likely predates the split of these major clades. The appendage morphology in the less well preserved Burgess Shale arthropod *Sanctacaris* (23) shows similarities to that in *Dibasterium* and *Offacolus* (8), but the origin of the biramous limb within early Paleozoic arthropods remains to be elucidated.

Methods

The holotype of *Dibasterium durgae* (OUMNH C.29640) was ground at 30 μm intervals, in three separate pieces. Surfaces were imaged digitally and image stacks used to generate a three-dimensional "virtual fossil" using the custom SPIERS software suite (www.spiers-software.org) (8, 24). The virtual fossil (Movie S1) was studied on-screen using the manipulation, virtual dissection, and stereoscopic-viewing capabilities of SPIERS. Images in Fig. 1 were rendered as ray-traced virtual photographs. The data are housed at the University Museum of Natural History, Oxford (OUMNH).

The holotype of *Dibasterium durgae* (OUMNH C.29640) was studied as an interactive virtual model, in VAXML format. VAXML models (25) consist of a series of STL- or PLY-format files describing morphology, together with an XML-based file providing metadata. The models can be imported into any 3D graphics package that supports STL/PLY files, or more conveniently can be viewed directly using the SPIERSview component of the freely available SPIERS software suite (www.spiers-software.org).

In order to understand the affinities of *Dibasterium* and its significance for arthropod evolution, this taxon and 36 other panarthropod exemplars were coded into a modified character set based on Rota-Stabelli et al. (26) (*SI Text*). A nexus file of this dataset is present in Dataset S1. Cladograms were computed using Traditional search options in TNT v.1.1. (27). To find the most parsimonious trees a tree bisection-reconnection (TBR) algorithm with 1,000 replicates and saving 100 trees per cycle was used. Characters were weighted using implied weighting (28) with a concavity constant (*k*) of 3. Multistate characters were unordered. Nodal support was measured with Symmetric Resampling (29), using 1,000 replicates and a heuristic search with a change probability of 33 per cent; these are reported as frequency differences between groups present and contradicted (i.e. GC). The result is presented in Fig. 2, Fig. S1.

ACKNOWLEDGMENTS. We thank R. Fenn, T. Hall, and J. Sinclair for general assistance; and G. A. Boxshall, J. Haug, and A. Monteiro for discussion and comments. We also thank the Natural Environment Research Council (grant NE/F017227/1) and the Yale Peabody Museum of Natural History Invertebrate Paleontology Division for support.

1. Shultz JW (2007) A phylogenetic analysis of the arachnid orders based on morphological characters. *Zool J Linn Soc Lond* 150:221–265.
2. Dunlop JA (2010) Geological history and phylogeny of Chelicerata. *Arthropod Struct Dev* 39:124–142.
3. Dunlop JA, Selden PA (1998) The early history and phylogeny of the chelicerates. *Arthropod Relationships*, eds RA Fortey and RH Thomas (Chapman and Hall, London), pp 221–235.
4. Anderson LI, Selden PA (1977) Opisthosomal fusion and phylogeny of Palaeozoic Xiphosura. *Lethaia* 30:19–31.
5. Van Roy P, et al. (2010) Ordovician faunas of Burgess Shale type. *Nature* 465:215–218.
6. Moore RA, McKenzie SC, Lieberman BS (2007) A Carboniferous synziphosurine (Xiphosura) from the Bear Gulch Limestone, Montana, USA. *Palaeontology* 50:1013–1019.
7. Orr PJ, Siveter Derek J, Briggs DEG, Siveter David J, Sutton MD (2000) A new arthropod from the Silurian Konservat-Lagerstätte of Herefordshire, England. *Proc R Soc Lond B* 267:1497–1504.
8. Sutton MD, Briggs DEG, Siveter David J, Siveter Derek J, Orr PJ (2002) The arthropod *Offacolus kingi* (Chelicerata) from the Silurian of Herefordshire, England: Computer based morphological reconstructions and phylogenetic affinities. *Proc R Soc Lond B* 269:1195–1203.
9. Moore RA, et al. (2005) A new synziphosurine (Chelicerata: Xiphosura) from the Late Llandovery (Silurian) Waukesha Lagerstätte, Wisconsin, USA. *J Paleont* 79:242–250.
10. Moore RA, Briggs DEG, Bartels C (2005) A new specimen of *Weinbergina opitzi* (Chelicerata: Xiphosura) from the Lower Devonian Hunsrück Slate, Germany. *Paläontol Z* 79:399–408.
11. Briggs DEG, Siveter David J, Siveter Derek J (1996) Soft-bodied fossils from a Silurian volcaniclastic deposit. *Nature* 382:248–250.
12. Briggs DEG, Siveter Derek J, Siveter David J, Sutton MD (2008) Virtual fossils from a 425 million-year-old volcanic ash. *Am Sci* 96:474–481.
13. Orr PJ, Briggs DEG, Siveter David J, Siveter Derek J (2000) Three-dimensional preservation of a non-biomineralized arthropod in concretions in Silurian volcaniclastic rocks from Herefordshire, England. *J Geol Soc Lond* 157:173–186.
14. Boxshall GA (2004) The evolution of arthropod limbs. *Biol Rev* 79:53–300.
15. Boxshall GA, Jaume D (2009) Exopodites, epipodites and gills in crustaceans. *Arth Syst Phyl* 67:229–254.
16. Jager M, et al. (2006) Homology of arthropod anterior appendages revealed by Hox gene expression in a sea spider. *Nature* 441:506–508.
17. Brenneis G, Ungerer P, Scholtz G (2008) The chelifores of sea spiders (Arthropoda, Pycnogonida) are the appendages of the deutocerebral segment. *Evol Dev* 10:717–724.
18. Mittmann B, Scholtz G (2001) *Distal-less* expression in embryos of *Limulus polyphemus* (Chelicerata, Xiphosura) and *Lepisma saccharina* (Insecta, Zygentoma) suggests a role in the development of mechanoreceptors, chemoreceptors, and the CNS. *Dev Genes Evol* 211:232–243.
19. Scholtz G, Mittmann B, Gerberding M (1998) The pattern of *Distal-less* expression in the mouthparts of crustaceans, myriapods and insects: New evidence of gnathobasic mandible and the common origin of Mandibulata. *Int J Dev Biol* 42:801–810.
20. Wolff C, Scholtz G (2008) The clonal composition of biramous and uniramous arthropod limbs. *Proc R Soc Lond B* 275:1023–1028.
21. Budd GE (1996) The morphology of *Opabinia regalis* and the reconstruction of the arthropod stem group. *Lethaia* 29:1–14.
22. Daley AC, Budd GE, Caron J-B, Edgecombe GD, Collins D (2009) The Burgess Shale anomalocaridid *Hurdia* and its significance for early euarthropod evolution. *Science* 323:1597–1600.
23. Briggs DEG, Collins D (1988) A Middle Cambrian chelicerate from Mount Stephen, British Columbia. *Palaeontology* 31:779–798.
24. Sutton MD, Briggs DEG, Siveter David J, Siveter Derek J (2001) Methodologies for the visualization and reconstruction of three-dimensional fossils from the Silurian Herefordshire Lagerstätte. *Palaeontol Electronica* 14, art. 1, 17 pp. http://palaeo-electronica.org/2001_1/s2/main.htm.
25. Sutton MD, Garwood RJ, Siveter David J, Siveter Derek J (2012) SPIERS and VAXML; a software toolkit for tomographic visualisation, and a format for virtual specimen interchange. *Palaeontol Electronica* 15, art. 5T, 14 pp. palaeo-electronica.org/content/issue-2-2012-technical-articles/226-virtual-palaeontology-toolkit.
26. Rota-Stabelli O, et al. (2011) A congruent solution to arthropod phylogeny: Phylogenomics, microRNAs and morphology support Mandibulata. *Proc Roy Soc Lond B* 278:298–306.
27. Goloboff PA, Farris JS, Nixon KC (2008) TNT, a free program for phylogenetic analysis. *Cladistics* 24:774–786.
28. Goloboff PA (1993) Estimating character weights during tree search. *Cladistics* 9:83–91.
29. Goloboff PA, et al. (2003) Improvements to resampling measures of group support. *Cladistics* 19:324–332.